JOURNAL OF GUIDANCE, CONTROL, AND DYNAMICS
Vol. 21, No. 1, January–February 1998

Multi-Pulse-Width Modulated Control of Linear Systems

Franco Bernelli-Zazzera,* Paolo Mantegazza,† and Vittorio Nurzia‡
Politecnico di Milano, 20133 Milan, Italy

A method is presented to convert a parent discrete time control into a multi-pulse-width modulated equivalent. It is shown that such an equivalence can be established by matching the system state response at each sampling interval and that, provided a sufficient number of pulses per sampling interval are used, the degree of approximation can be as high as desired even if a relatively slow sampling frequency is adopted. A numerical example on a simple fourth-order system provides the basis for understanding the pros and cons of the method, which is then applied to a more complex aerospace problem: the stabilization of coupled thermoelastic vibrations of a space structure.

I. Introduction

MANY control systems use actuators that are discontinuously operated among a limited number of outputs, mostly two or three states. Among aerospace applications, typical examples are the jet thrusters used for attitude and/or shape control of spacecraft,[1] which can produce either a constant or null force.

This operating mode leads to a controller implementing a simple switching rule but introduces a high nonlinearity in the controlled system and, generally, there can be no nonzero steady state but a limit cycle periodic response. Nonetheless, if a sufficiently fast sampling rate is adopted, even the strictest requirements can be satisfied. There are, however, some limitations to their application that are difficult to overcome, e.g., when a significant actuating power must be transferred mechanically between moving parts in contact and it is not possible to limit their wearing rate to an acceptable level or if stringent specifications are set on state derivatives.

Except for the simplest control tasks, when high switching frequencies can be adopted, to obtain good performances from an on/off or bang-bang actuator, it is necessary to design the appropriate switching law by means of a generally burdensome, nonlinear control design technique. The most used design methods are variable structure theory[2–5] and pulse width and/or pulse frequency modulation (PWM-PWPFM).[6]

A review of pulse width and/or pulse frequency modulators can be found in Ref. 7 together with a number of other references regarding practical applications of the reported techniques. Some interesting aerospace applications of pulse width modulated controls are presented in Refs. 8–10. In Ref. 11, a standard linear continuous time invariant multi-input system is modified to allow a general modeling of two states pulsewidth modulated actuators in such a way that only the average of the actuator output can be zero within each sampling interval. This approach does not allow stabilization of an unstable system and, lacking the off state, could lead to a useless waste of control power.

Another way to carry out the design of the control system is proposed in Ref. 12, where an equivalence is set between a pulse width modulated control law and a parent discrete-time control, hereafter called pulse amplitude modulation (PAM), for which a wide variety of well-known and widely used design techniques exist. This is accomplished by imposing the equality of the areas under the two control implementations within each sampling interval, in such a way that an optimal firing delay can be determined by minimizing the norm of the error between the PAM and its equivalent PWM responses. This is a very powerful approach because it allows the designer to ignore the nonlinear actuators even when relatively long sampling times are used. Because the PAM to PWM conversion is based on the equivalence between responses to corresponding input histories, the method would work not only for control inputs but also for any arbitrary command sequence.

In a more recent paper it is shown that a first-order PAM to PWM equivalence can be obtained by a single maximum amplitude PWM impulse, centered within the sampling interval, having an area equal to that of the parent PAM input.[13]

In this paper we present a way to further improve the equivalence by allowing more than one pulse to appear within each sampling interval. The resulting controller, hereafter called multi-pulse-width modulated (MPWM), is a true PWM system, because the amplitude of the control is either zero or at plus–minus on states, but with pulses unequally spread over the sampling interval. At first glance MPWM control can also be interpreted as a more traditional PWPFM control, but it must be immediately clear that the two methods rely on completely different assumptions and design techniques. In fact, the PWPFM synthesis relies mostly on frequency-domain analyses of single-input/single-output systems, whereas MPWM synthesis can be carried out by using any design methodology for general multivariable systems, either in the time or frequency domain. Therefore MPWM controllers can benefit from any improvement in control design theory. From a practical point of view, detailed in the sequel of the paper, the pulsed controller represents a translation of an equivalent discrete time control, which does not require the knowledge of the system model. This means that the extra computational burden required to perform the translation is very limited even for complex systems and does not impede the possibility of evaluating very complicated control laws in real time.

Two simulated applications are then presented to demonstrate the obtainable performances.

II. Problem Formulation

The system to be controlled is assumed to be linear and is governed by the standard set of time invariant differential equations

$$\dot{\boldsymbol{x}} = \boldsymbol{A}\boldsymbol{x} + \boldsymbol{B}\boldsymbol{u} \tag{1}$$

where $\boldsymbol{A}$ and $\boldsymbol{B}$ are constant matrices, $\boldsymbol{x} \in \Re^n$ and $\boldsymbol{u} \in \Re^m$, whose solution is

$$\boldsymbol{x}(t+\Delta) = e^{\boldsymbol{A}\Delta}\boldsymbol{x}(t) + \int_t^{t+\Delta} \exp[\boldsymbol{A}(t+\Delta-\eta)]\boldsymbol{B}\boldsymbol{u}(\eta)\,\mathrm{d}\eta \tag{2}$$

We want to compare the following two situations (Fig. 1): 1) discrete PAM control: the input is constant over the sampling period

$$u_j^{(\mathrm{PAM})}(\eta) = u_j(k\Delta) \qquad \text{for} \qquad k\Delta \le \eta < (k+1)\Delta \tag{3}$$

and 2) MPWM control: the input is either zero or the maximum

$$u_j^{(\mathrm{PWM})}(\eta) = \begin{cases} u_{Mj} & \text{if} \quad k\Delta + T_{ji} - \delta_{ji} \le \eta < k\Delta + T_{ji} \\ 0 & \text{otherwise} \end{cases} \tag{4}$$

where Δ is the sampling period, u_j is the jth entry of the input vector ($j = 1, 2, \ldots, m$), and δ_{ji} and T_{ji} are the duration and the

---

Received May 13, 1996; revision received July 21, 1997; accepted for publication Aug. 15, 1997.

*Associate Professor, Department of Aerospace Engineering, Via Golgi 40. Member AIAA.

†Professor, Department of Aerospace Engineering, Via Golgi 40.

‡Graduate Student, Department of Aerospace Engineering, Via Golgi 40.

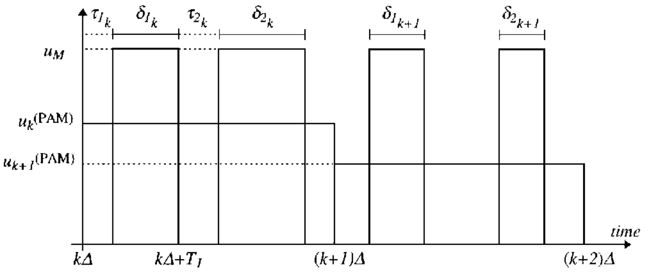

Fig. 1 PAM/MPWM transformation.

final time instants of the ith pulse of the jth input, respectively. Introducing the delay τ_{ji} between the end of the $(i-1)$th pulse and the beginning of the ith pulse of the jth input, for a sequence of p pulses for each input, we can write

$$T_{ji} = \sum_{h=1}^{i} (\tau_{jh} + \delta_{jh}), \qquad i = 1, 2, \ldots, p, \quad j = 1, 2, \ldots, m \tag{5}$$

To introduce an equivalence between control laws (3) and (4), we have to develop the integral of Eq. (2) in a form so as to make evident the pulse parameters T_{ji} and δ_{ji}. Because of the possibility of applying the superposition principle in the sequel we will, for sake of conciseness, refer to a single-input system, i.e., $\boldsymbol{B} = \boldsymbol{b} \in \Re^{\eta}$.

Substituting Eqs. (3) and (4) into Eq. (2) and calling $\boldsymbol{x}_f$ the forced part of the discrete time state vector, which is the only one affected by the input and whose expression is

$$\boldsymbol{x}_f(k\Delta + \Delta) = \int_{k\Delta}^{k\Delta+\Delta} \exp[\boldsymbol{A}(k\Delta + \Delta - \eta)]\boldsymbol{b}u(\eta)\,\mathrm{d}\eta \tag{6}$$

we obtain

$$\boldsymbol{x}_f^{(\mathrm{PAM})}(k\Delta + \Delta) = \left[\int_{k\Delta}^{k\Delta+\Delta} \exp[\boldsymbol{A}(k\Delta + \Delta - \eta)]\,\mathrm{d}\eta\right]\boldsymbol{b}u_k \tag{7}$$

$$\boldsymbol{x}_f^{(\mathrm{PWM})}(k\Delta + \Delta) = \left[\sum_{i=1}^{p}\int_{T_i-\delta_i}^{T_i} \exp[\boldsymbol{A}(k\Delta + \Delta - \eta)]\,\mathrm{d}\eta\right]\boldsymbol{b}u_M \tag{8}$$

Using a Taylor expansion for the matrix exponential and performing the integrals, we are lead to the following relations:

$$\boldsymbol{x}_f^{(\mathrm{PAM})}(k\Delta + \Delta) = \left[\sum_{j=0}^{\infty}\frac{\boldsymbol{A}^j\Delta^{j+1}}{(j+1)!}\right]\boldsymbol{b}u_k = \Psi(\Delta)\boldsymbol{b}u_k \tag{9}$$

$$\begin{aligned}\boldsymbol{x}_f^{(\mathrm{PWM})}(k\Delta + \Delta) &= \sum_{i=1}^{p}[\boldsymbol{\Psi}(\Delta - T_i + \delta_i) - \boldsymbol{\Psi}(\Delta - T_i)]\boldsymbol{b}u_M \\ &= \left\{\sum_{j=0}^{\infty}\frac{\boldsymbol{A}^j}{(j+1)!}\sum_{i=1}^{p}\left[(\Delta - T_i + \delta_i)^{j+1}\right.\right. \\ &\qquad \left.\left. - (\Delta - T_i)^{j+1}\right]\right\}\boldsymbol{b}u_M\end{aligned} \tag{10}$$

The error between the two different responses is

$$\begin{aligned}\varepsilon_k = \sum_{j=0}^{\infty}\frac{\boldsymbol{A}^{j+1}\boldsymbol{b}}{(j+1)!}&\left\{\Delta^{j+1}u_k - \sum_{i=1}^{p}\left[(\Delta - T_i + \delta_i)^{j+1}\right.\right. \\ &\left.\left. - (\Delta - T_i)^{j+1}\right]u_M\right\}\end{aligned} \tag{11}$$

and can be seen as a series of infinite terms, where for each of them the factor affected by the shape of the MPWM input is clearly evidenced. Because the pulses are p and, for each pulse, two characteristic quantities, T_i and δ_i, are needed to correctly operate the actuator, we are able to determine p-pulses shaped input so as to set the first $2p$ terms of the error to zero, by satisfying the following set of $2p$ nonlinear algebraic equations in the unknowns T_i and δ_i:

$$\Delta^{j+1}\frac{u_k}{u_M} = \sum_{i=1}^{p}\left[(\Delta - T_i + \delta_i)^{j+1} - (\Delta - T_i)^{j+1}\right]$$
$$j = 0, 1, 2, \ldots, 2p-1 \tag{12}$$

Note that the first equation ($j = 0$) can be written as

$$u_k\Delta = u_M\sum_{i=1}^{p}\delta_i \tag{13}$$

and, no matter how many pulses are present in the sampling interval, always states that the area under the PAM and MPWM input histories, i.e., their pulses over the sampling interval, must be equal.

The residual error now can be written as

$$\begin{aligned}\varepsilon_k = \sum_{j=2p}^{\infty}\frac{\boldsymbol{A}^{j+1}\boldsymbol{b}}{(j+1)!}&\left\{\Delta^{j+1}u_k - \sum_{i=1}^{p}\left[(\Delta - T_i + \delta_i)^{j+1}\right.\right. \\ &\left.\left. - (\Delta - T_i)^{j+1}\right]u_M\right\}\end{aligned} \tag{14}$$

which is a decreasing function of the number of pulses p. We will say that we set a $(2p-1)$th-order equivalence between the PAM and PWM inputs when the first nonzero term in the series that defines the error between the joint responses depends on the $2p$th power of the error.

For example, if we are interested in a first-order equivalence ($p=1$), it is easy to obtain the following solution:

$$\delta = \Delta(u_k/u_M), \qquad T = (\Delta + \delta)/2 \tag{15}$$

i.e., the single-pulse centered equivalence presented in Ref. 13.

If, instead, we want to set up a third-order equivalence ($p = 2$), the following set of nonlinear algebraic equations are to be solved:

$$\begin{aligned}\Delta(u_k/u_M) &= (\Delta - T_1 + \delta_1) - (\Delta - T_1) \\ &\quad + (\Delta - T_2 + \delta_1) - (\Delta - T_2) = \delta_1 + \delta_2 \\ \Delta^2(u_k/u_M) &= (\Delta - T_1 + \delta_1)^2 - (\Delta - T_1)^2 \\ &\quad + (\Delta - T_2 + \delta_2)^2 - (\Delta - T_2)^2 \\ \Delta^3(u_k/u_M) &= (\Delta - T_1 + \delta_1)^3 - (\Delta - T_1)^3 \\ &\quad + (\Delta - T_2 + \delta_2)^3 - (\Delta - T_2)^3 \\ \Delta^4(u_k/u_M) &= (\Delta - T_1 + \delta_1)^4 - (\Delta - T_1)^4 \\ &\quad + (\Delta - T_2 + \delta_2)^4 - (\Delta - T_2)^4\end{aligned} \tag{16}$$

which may also be written as

$$\Delta(u_k/u_M) = \delta_1 + \delta_2$$
$$\Delta^2(u_k/u_M) = 2(\Delta - T_1)\delta_1 + \delta_1^2 + 2(\Delta - T_2)\delta_2 + \delta_2^2$$
$$\begin{aligned}\Delta^3(u_k/u_M) &= 3(\Delta - T_1)^2\delta_1 + 3(\Delta - T_1)\delta_1^2 + \delta_1^3 \\ &\quad + 3(\Delta - T_2)^2\delta_2 + 3(\Delta - T_2)\delta_2^2 + \delta_2^3 \\ \Delta^4(u_k/u_M) &= +4(\Delta - T_1)^3\delta_1 + 6(\Delta - T_1)^2\delta_1^2 \\ &\quad + 4(\Delta - T_1)\delta_1^3 + \delta_1^4 + 4(\Delta - T_2)^3\delta_2 \\ &\quad + 6(\Delta - T_1)^2\delta_2^2 + 4(\Delta - T_1)\delta_2^3 + \delta_2^4\end{aligned} \tag{17}$$

In general, for orders of equivalence greater than one, we have to solve Eq. (12), typically with a Newton–Raphson method, which in this particular case takes the following recursive form:

$$\boldsymbol{v}_{h+1} = \boldsymbol{v}_h - \boldsymbol{G}_h^{-1}\boldsymbol{e}_h \tag{18}$$

where

$$
\boldsymbol{v}_h = \begin{Bmatrix} T_1^{(h)} \\ \delta_1^{(h)} \\ \vdots \\ T_p^{(h)} \\ \delta_p^{(h)} \end{Bmatrix}, \qquad \boldsymbol{e}_h = \begin{Bmatrix} \displaystyle\sum_{i=1}^{p} \delta_i^{(h)} - \Delta \frac{u_k}{u_M} \\ \vdots \\ \displaystyle\sum_{i=1}^{p} \Big[\big(\Delta - T_i^{(h)} + \delta_i^{(h)}\big)^{2p} - \big(\Delta - T_i^{(h)}\big)^{2p} \Big] - \Delta^{2p} \frac{u_k}{u_M} \end{Bmatrix}
$$

$$
\boldsymbol{G}_h = \begin{bmatrix} 0 & 1 & \cdots \\ -2\delta_1^{(h)} & 2\big(\Delta - T_1^{(h)} + \delta_1^{(h)}\big) & \cdots \\ \vdots & \vdots & \ddots \\ -2p\Big[\big(\Delta - T_1^{(h)} + \delta_1^{(h)}\big)^{2p-1} - \big(\Delta - T_1^{(h)}\big)^{2p-1}\Big] & 2p\big(\Delta - T_1^{(h)} + \delta_1^{(h)}\big)^{2p-1} & \cdots \end{bmatrix} \tag{19}
$$

For example, for a two-pulse modulator, the Newton–Raphson algorithm would use the following matrices:

$$
\boldsymbol{e}_h = \begin{Bmatrix} \delta_1^{(h)} + \delta_2^{(h)} - \Delta(u_k/u_M) \\ \big(\Delta - T_1^{(h)} + \delta_1^{(h)}\big)^2 - \big(\Delta - T_1^{(h)}\big)^2 + \big(\Delta - T_2^{(h)} + \delta_2^{(h)}\big)^2 - \big(\Delta - T_2^{(h)}\big)^2 - \Delta^2(u_k/u_M) \\ \big(\Delta - T_1^{(h)} + \delta_1^{(h)}\big)^3 - \big(\Delta - T_1^{(h)}\big)^3 + \big(\Delta - T_2^{(h)} + \delta_2^{(h)}\big)^3 - \big(\Delta - T_2^{(h)}\big)^3 - \Delta^3(u_k/u_M) \\ \big(\Delta - T_1^{(h)} + \delta_1^{(h)}\big)^4 - \big(\Delta - T_1^{(h)}\big)^4 + \big(\Delta - T_2^{(h)} + \delta_2^{(h)}\big)^4 - \big(\Delta - T_2^{(h)}\big)^4 - \Delta^4(u_k/u_M) \end{Bmatrix} \tag{20}
$$

$$
\boldsymbol{G}_h = \left[\begin{array}{c:c:c:c} 0 & 1 & 0 & 1 \\ \hdashline -2\delta_1^{(h)} & 2\big(\Delta - T_1^{(h)} + \delta_1^{(h)}\big) & -2\delta_2^{(h)} & 2\big(\Delta - T_2^{(h)} + \delta_2^{(h)}\big) \\ \hdashline -3\Big[\big(\Delta - T_1^{(h)} + \delta_1^{(h)}\big)^2 - \big(\Delta - T_1^{(h)}\big)^2\Big] & 3\big(\Delta - T_1^{(h)} + \delta_1^{(h)}\big)^2 & -3\Big[\big(\Delta - T_2^{(h)} + \delta_2^{(h)}\big)^2 - \big(\Delta - T_2^{(h)}\big)^2\Big] & 3\big(\Delta - T_2^{(h)} + \delta_2^{(h)}\big)^2 \\ \hdashline -4\Big[\big(\Delta - T_1^{(h)} + \delta_1^{(h)}\big)^3 - \big(\Delta - T_1^{(h)}\big)^3\Big] & 4\big(\Delta - T_1^{(h)} + \delta_1^{(h)}\big)^3 & -4\Big[\big(\Delta - T_2^{(h)} + \delta_2^{(h)}\big)^3 - \big(\Delta - T_2^{(h)}\big)^3\Big] & 4\big(\Delta - T_2^{(h)} + \delta_2^{(h)}\big)^3 \end{array}\right] \tag{21}
$$

A good initial guess for the iterative process can be obtained either by subdividing the sample interval into p equal parts and then applying the first-order solution to each subinterval or by taking it from the preceding control step. The latter choice is based on the assumption that excessively large variations of the input rarely occur and cannot be used when the control inputs saturate.

Extended simulations have proved that a small relative error can be achieved in very few iterations, so that the related computational load should not add any significant computational cost. However, it must be noted that the equivalence thus established is based on the assumption of identical initial conditions at each sampling point. This is obviously not possible because at the end of each sampling time the resulting PWM state vector is different from the one obtainable by means of a PAM control law, and the error propagates from one sampling interval to the next one. Note that nothing can be said about the difference in the system response in the case of nonperfect matching. In some cases a low number of pulses may generate an unpredicted (even if different from its parent PAM) improved time response.

Nevertheless, it will be shown that increasing the order of the equivalence increases the similarity between the entire PAM and MPWM time histories.

If the input gets saturated, the equivalence between the PAM and the MPWM responses is trivial and degenerates in a single pulse covering the whole sampling interval ($T = \delta = \Delta$).

Because of the relative ease in designing good PAM control laws, the ability to improve the equivalence between PAM and PWM responses without reducing the sampling rate can be of paramount importance in those applications in which complex centralized and computer thirsty digital controllers must be implemented. In fact, if a simpler equivalence is used, i.e., a single pulse centered within the sampling interval,[13] a faster sampling inevitably would be required to achieve the same performances obtainable with a MPWM. Thus, if constraints are posed on the performances of the hardware to be used, complex control laws cannot be implemented, whereas it is likely instead that, due to its low added computational cost, the MPWM will make possible a precise equivalence with the available computational resources.

Note that relatively fast firings are assumed in determining the MPWM equivalence, but this should not hinder its practical applications as a not-as-fast firing will limit the performances of the equivalent implementation only when the controller is close to saturation. Instead, when the duty cycle is below saturation, the off times will be wide enough to allow the compensation of delays in achieving fully an output by appropriate anticipation of the firing times. An alternate approach is to model the dynamics of the actuators, bringing the firings as close as possible to their fast switching logic.

III. Applications

Two examples are studied to investigate the possibility of taking advantage of the method just discussed. They are closely related to those presented in Ref. 7 and cover the applications to different operating frequencies.

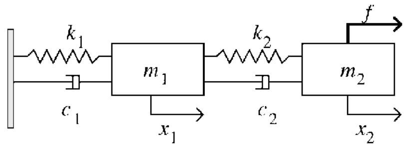

Fig. 2 Mass–spring–damper system.

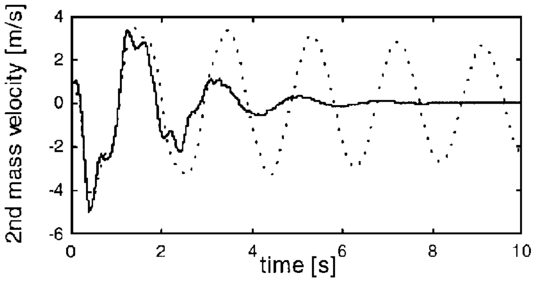

a) Free and PWM controlled response

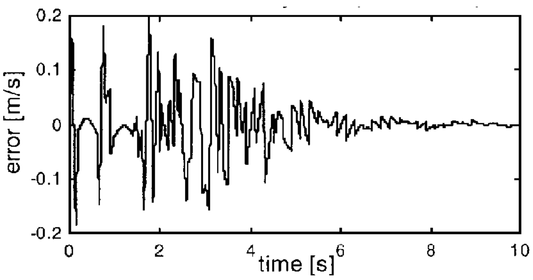

b) Second mass velocity error (PAM-PWM)

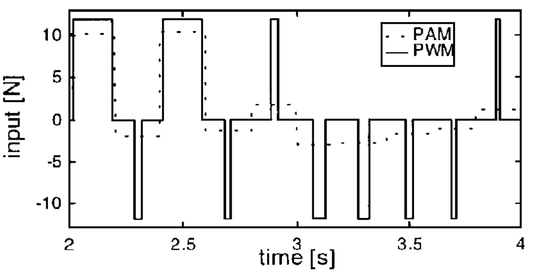

c) Control action

Fig. 3 PAM/PWM equivalence (single centered pulse).

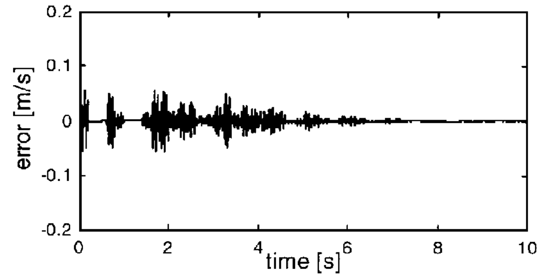

a) Second mass velocity error (PAM-PWM)

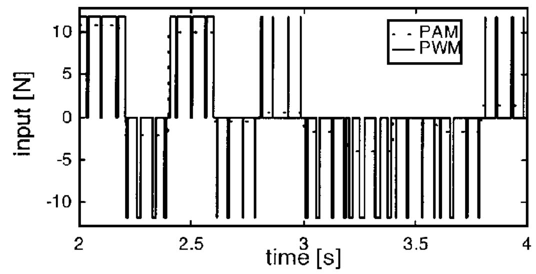

b) Control action

Fig. 4 PAM/MPWM equivalence (four pulses).

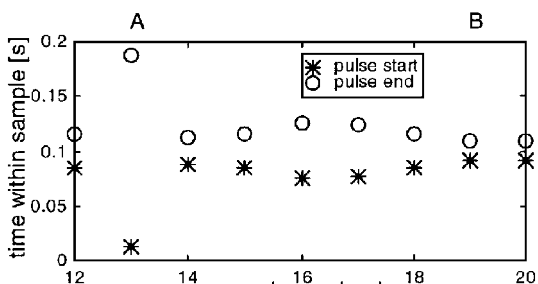

a)

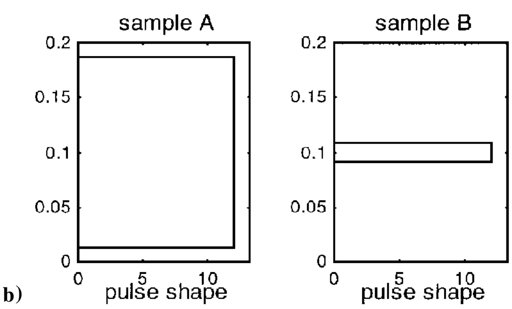

b)

Fig. 5 PWM control sample (one pulse).

A. Example 1: Mass–Spring–Damper System

The first example is somewhat abstract and is a typical vibratory system, like the one shown in Fig. 2, in which the actuator is a constant force jet thruster. The parameters m_1, m_2, k_1, k_2, c_1, and c_2 were selected in such a way that the resulting linear system (1) had the natural frequencies of 0.52 and 1.76 Hz and damping of 0.012 and 0.05, respectively. Then a full state controller was designed by pole placement so as to increase the damping factor to 0.2 for both natural modes, leaving the frequencies unaltered. The input force level is set to ± 12 N, a value selected to match the desired closed-loop behavior with both no actuator saturation and a well-used control power. The control frequency was set to 5 Hz, i.e., just three times the highest frequency to be controlled.

Figures 3 and 4 show the performances of MPW modulators with a single pulse and four pulses. For conciseness the comparison between the free and controlled responses is shown only in Fig. 3a. Figures 3b and 3c present the mean square error between the PAM and MPWM responses and the control activity related to p pulses.

Figures 5 and 6 report a sample of the control action of two modulators. Figures 5a and 6a represent the starting and ending instants for each pulse appearing in the sampling interval. The actual pulse width modulated control shapes for two sampling intervals are in Figs. 5b and 6b; they may be viewed as sections of Figs. 5a and 6a. In each graph the vertical axis limit is the actual sampling time. It is evident that neither the optimal positions of the pulses obtained from the iteration are at the center of each subinterval nor are the pulse widths equal.

In all of the cases the control action of the MPWM regulator is very effective and quite similar to its PAM parents. Table 1 makes it evident that the MPWM/PAM error is subject to a significant decrease when passing from a single to a two-pulse modulator, whereas higher-order equivalents do not produce further significant improvements. This is not surprising because the order of equivalence is referred to the powers of the sampling intervals.

In Fig. 7, the evolution of the number of iterations during the simulation is shown for the cases of two-, three-, and four-pulse modulators. It is recalled that the single pulse does not require an iterative solution. In each plot, the results related to both the mentioned initial guesses are reported. In all cases, it is clear that the recursive algorithm converges after a few iterations and how the initial solution based on the previous control step allows a faster convergence. It is noted that, when the input is saturated, no iteration is required because only a single pulse is applied covering the entire sampling interval, so that the subsequent solution must be

Table 1 MPWM/PAM average errors

One pulse	Two pulses	Three pulses	Four pulses
2.032e-02	7.874e-04	5.515e-04	4.330e-04

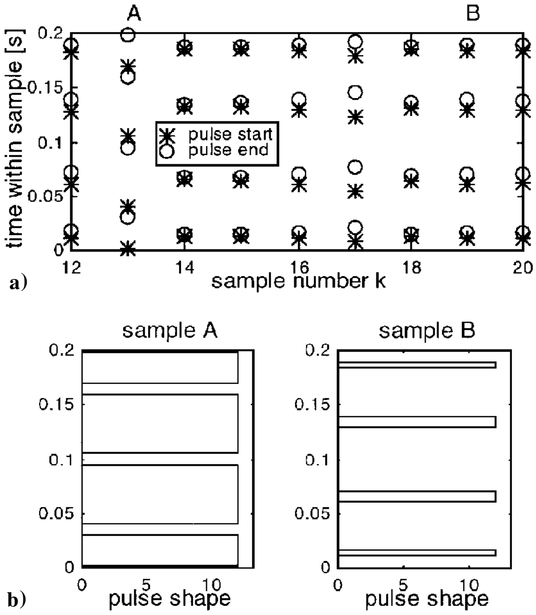

Fig. 6 MPWM control sample (four pulses).

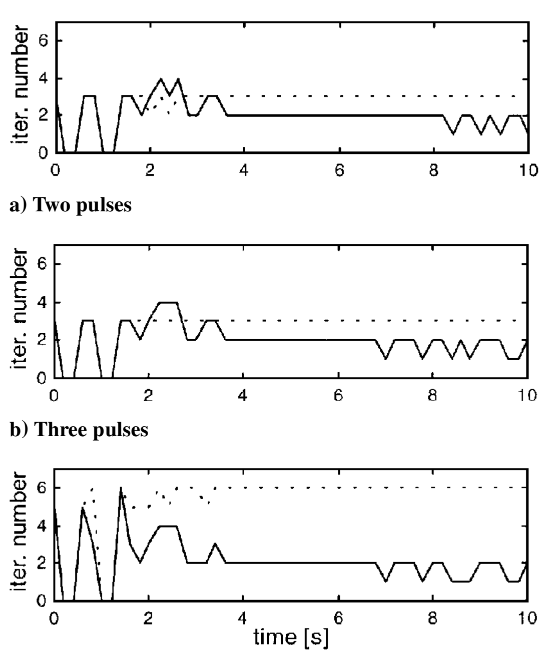

a) Two pulses

b) Three pulses

c) Four pulses

Fig. 7 Number of iterations in the Newton–Raphson algorithm: · · · · ·, initial guess based on equicentered pulses and ——, initial guess based on the results of the preceding time step.

evaluated by starting from the first-order equivalent, and the number of iterations following a saturated input is always higher than in other conditions.

Finally, Fig. 8 gives an intuitive representation of how the different modulators work and why, physically speaking, the higher the number of pulses the better the equivalence is. The second mass velocity appears with the typical sawtooth behavior of a PWM input response; it is evident that, as the number of pulses per sampling interval increases, the response oscillations become more frequent but their amplitudes decrease.

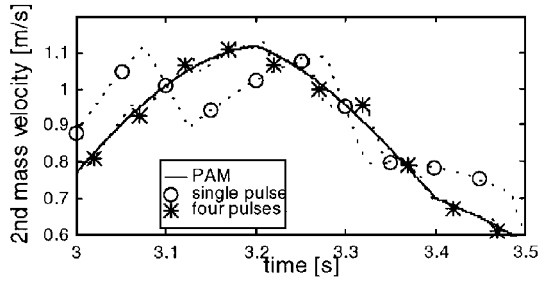

Fig. 8 Behavior of the PWM devices: PAM vs PWM.

This simple example leads to the following considerations.

1) The method works as expected: the control designer is required to synthesize a standard discrete time PAM regulator without taking into account the nonlinear behavior of the actuators. In the implementation phase, the PAM to MPWM conversion is easily inserted only as a translation algorithm.

2) A relatively large number of pulses per sampling interval may not bring a very high improvement in controller performances; one has to consider each practical application to verify which modulator is a faithful enough translator of the PAM control law.

B. Example 2: Control of Thermally Induced Vibrations on a Flexible Boom

This example is a real, challenging, aerospace application, in which the controller must operate at low frequencies due to the usually lower computational capability of space qualified computers. Thus, the chance of designing relatively complex PAM regulators and implementing them in an equivalent MPWM form becomes interesting.

Example 2 deals with the application of an MPWM controller to an unstably coupled thermoelastic structural system, in which the heating input depends on the actual structural shape resulting from thermally induced displacements. This leads to a thermostructural feedback that can cause unstable vibrations of a slender flexible boom in space. It represents a challenging test for a variety of reasons, inasmuch as the system is multivariable, unstable, and the control action is either unidirectional or zero.

The structure under test represents a simplified model of the boom of the OGO-IV spacecraft, which was known to be affected by sustained oscillations related to the crossing from the Earth's shadow into sunlight and vice versa. Various analytical methods to study thermally induced oscillations have been proposed. For the control problem, a detailed presentation of a coupled thermoelastic model, based on the formulation of Ref. 14, can be found in Refs. 15 and 16, where it is shown that the system can be represented in the state-space form as

$$\begin{Bmatrix} \ddot{\boldsymbol{q}} \\ \dot{\boldsymbol{q}} \\ \dot{\boldsymbol{h}} \end{Bmatrix} = \begin{bmatrix} -2\Xi\Omega & -\Omega^2 & \Phi^T Z\Theta \\ \boldsymbol{I} & \boldsymbol{0} & \boldsymbol{0} \\ \boldsymbol{0} & \Theta^T\Gamma & -\Lambda \end{bmatrix} \begin{Bmatrix} \dot{\boldsymbol{q}} \\ \boldsymbol{q} \\ \boldsymbol{h} \end{Bmatrix} + \begin{bmatrix} \boldsymbol{0} \\ \boldsymbol{0} \\ \Theta^T \end{bmatrix} \boldsymbol{u} + \begin{Bmatrix} \boldsymbol{0} \\ \boldsymbol{0} \\ \Theta^T \boldsymbol{P}^* \end{Bmatrix} \tag{22}$$

where $\boldsymbol{q}$ and $\boldsymbol{h}$ are the generalized structural and thermal modal coordinates; Φ and Θ the structural and thermal mode shapes; Z and Γ the thermoelastic and elastothermal coupling terms; and Ω, Ξ, and Λ the structural natural frequencies, damping factors, and thermal eigenvalues matrices; also, $\boldsymbol{u}$ is the control vector of the thermal loads and $\boldsymbol{P}^*$ the part of sunlight thermal input, which does not depend on the structure displacements.

The structural and thermal modes are evaluated on a double finite element model (Fig. 9), one for the structural displacements and one for the temperature distribution, which are only requested to be interfaceable, i.e., the two models must have some common grid points but not necessarily the same connections between these points.

Table 2 Eigenvalues of the flexible boom model

Mode number and shape	Uncoupled		Coupled	
	Real	Imaginary	Real	Imaginary
1st structural	0.0	±1.28	±1.5e-04	±1.28
10th structural	0.0	±31.8	−1.4e-05	±31.8
1st thermal	−0.654	0.0	−0.654	0.0
38th thermal	−0.658	0.0	−0.658	0.0

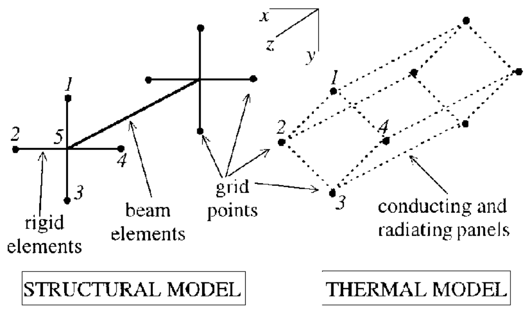

Fig. 9 Finite element models of the flexible boom.

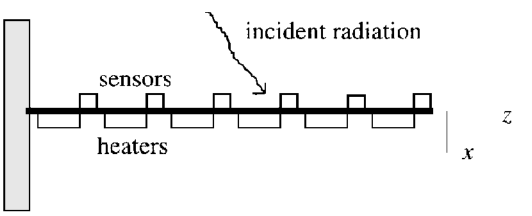

Fig. 10 Layout of the flexible boom control system.

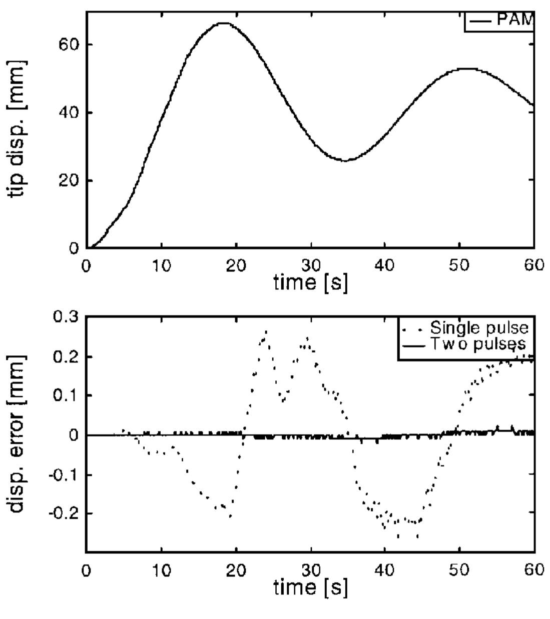

Fig. 11 Flexible boom–tip displacement PAM/MPWM responses and errors.

Table 2 reports the slowest and fastest structural and thermal eigenvalues used in Eq. (22) and how these eigenvalues are modified by the coupling effects. The thermal eigenvalues are hardly affected by the coupling and, neglecting any structural damping, the lowest structural modes become unstable due to the thermal coupling.

The control makes use of six equally spaced sensors and actuators, positioned along the structure, as shown in Fig. 10. It is assumed that the sensors measure local displacements and velocities or allow their easy and fast reconstruction so that the observed dynamics need not be modeled, while the actuators are heating layers placed on the shaded surface of the boom. Each actuator is driven only by its nearest sensor, in a fully decentralized and collocated control

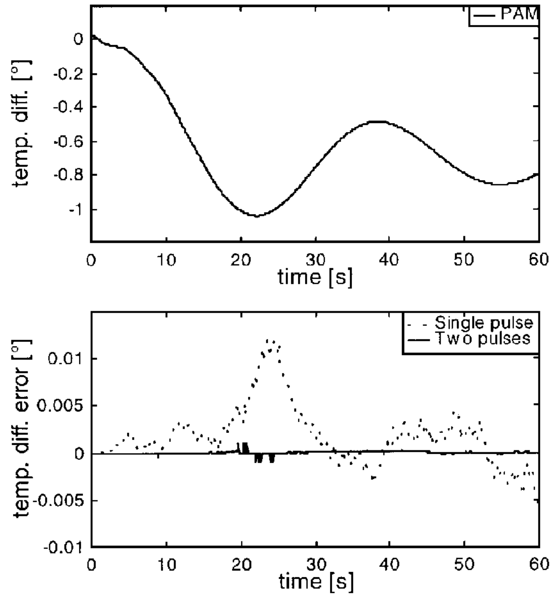

Fig. 12 Flexible boom–temperature difference PAM/MPWM responses and errors.

scheme. The main drawback of such a thermal control, in terms of actuator complexity, is represented by the necessity of cooling, so that a purely heating control law appears highly desirable. This is achieved, for each heater, with a control law of the kind

$$u = K_x m_x + K_{\dot{x}} m_{\dot{x}} + r \tag{23}$$

where the constant feedforward vector r is chosen in such a way as to eliminate the temperature difference between the sunlit and shaded surfaces (nodes 4 and 2 in Fig. 9) in the uncontrolled case.

The controller was designed with reference to the discrete equivalent of Eq. (22), sampled at 20 Hz, supposing each heater is capable of transmitting up to 15 W to the structure.

Modulators of orders 1–3 were implemented, determining that a two-pulse modulator is very convenient to guarantee a better equivalence between PAM and PWM responses and, as a consequence, a higher confidence in designing the controller as a discrete feedback (23). The controlled responses, referred to their PAM parents, are shown in Figs. 11 and 12.

This example shows how the method presented can be employed in an actual application. It is important to stress that the algorithm does not affect the control system design, but it just guarantees that the PAM controller performances are achieved with PWM actuators having an assigned order of equivalence.

IV. Concluding Remarks

The paper has presented a method to translate discrete time pulse amplitude modulated control laws in such a way that equivalent performances can be obtained by using multi-pulse-width modulated actuators. This leads to a convenient and viable way to implement active control systems using highly nonlinear actuators while the design can be easily and effectively carried out using discrete time control methodologies.

Out of a large number of numerical verifications, two examples of different complexity have been used to demonstrate the effectiveness of the proposed technique. The simulations were aimed at verifying whether using more than one impulse in each sampling interval could lead, as theoretically expected, to an increased level of confidence in the PAM/MPWM responses equivalence and whether this task could be accomplished with reasonable added computational cost and control algorithm complexity.

No major limitations in the applicability of the technique were found, and an experimental verification of the method is being designed.

The most promising applications of the presented methodology are likely to be found in on–off low-frequency controls, typical and often compulsory in many aerospace systems, for which a multi-pulse conversion can be much more precise than a single-pulse equivalence.

References

[1]Sutton, G. P., *Rocket Propulsion Elements: An Introduction to the Engineering of Rockets*, Wiley, New York, 1986.

[2]Itkis, U., *Control Systems of Variable Structure*, Wiley, New York, 1976.

[3]Utkin, V. I., "Variable Structure Systems with Sliding Modes," *IEEE Transactions on Automatic Control*, Vol. AC-22, No. 2, 1977, pp. 212–222.

[4]Utkin, V. I., and Yang, K. D., "Methods for Constructing Discontinuity Planes in Multidimensional Variable Structure Systems," *Automation and Remote Control*, 1979, pp. 1466–1470.

[5]Utkin, V. I., *Sliding Mode in Control Optimization*, Springer–Verlag, Berlin, 1992.

[6]Skoog, R. A., and Blankenship, G. L., "Generalized Pulse-Modulated Feedback Systems: Norms, Gains, Lipshitz Constants and Stability," *IEEE Transactions on Automatic Control*, Vol. AC-21, 1970, pp. 300–315.

[7]Bernelli-Zazzera, F., and Mantegazza, P., "Linearization Techniques for Pulse Width Control of Linear Systems," *Control and Dynamic Systems*, Vol. 70, 1995, pp. 67–111.

[8]Wie, B., and Plescia, C. T., "Attitude Stabilization of Flexible Spacecraft During Stationkeeping Maneuvers," *Journal of Guidance, Control, and Dynamics*, Vol. 7, No. 4, 1984, pp. 430–436.

[9]Anthony, T. C., Wie, B., and Carroll, S., "Pulse Modulated Control Synthesis for a Flexible Structure," *Proceedings of the AIAA Guidance, Navigation, and Control Conference* (Boston, MA), AIAA, Washington, DC, 1989, pp. 65–76.

[10]Skaar, S. B., Tang, L., and Yalda-Mooshabad, I., "On–Off Attitude Control of Flexible Satellites," *Journal of Guidance, Control, and Dynamics*, Vol. 9, No. 4, 1986, pp. 507–510.

[11]Friedland, B., "Modeling Linear Systems for Pulsewidth Modulated Control," *IEEE Transactions on Automatic Control*, Vol. AC-21, No. 5, 1976, pp. 739–746.

[12]Bernelli-Zazzera, F., and Mantegazza, P., "Pulse Width Equivalent to Pulse Amplitude Discrete Control of Linear Systems," *Journal of Guidance, Control, and Dynamics*, Vol. 15, No. 2, 1992, pp. 461–467.

[13]Shieh, L. S., Wang, W. M., and Sunkel, J. W., "Design of PAM and PWM Controllers for Sample-Data Internal Systems," *Journal of Dynamic Systems, Measurement and Control* (to be published).

[14]Frish, H. P., "Thermally Induced Response of Flexible Structures: a Method for Analysis," *Journal of Guidance, Control, and Dynamics*, Vol. 3, No. 1, 1980, pp. 92–94.

[15]Bernelli-Zazzera, F., Ercoli-Finzi, A., and Mantegazza, P., "Thermoelastic Behavior of Large Space Structures: Modeling and Control," *Proceedings of the International Conference on Spacecraft Structures and Mechanical Testing*, ESA SP-289, European Space Agency, Noordwijk, The Netherlands, 1988, pp. 195–200.

[16]Bernelli-Zazzera, F., Ercoli-Finzi, A., and Mantegazza, P., "Control Strategies for Thermally Induced Vibrations of Space Structures," *Proceedings of the 7th VPI&SU Symposium on Dynamics and Control of Large Structures* (Blacksburg, VA), 1989, pp. 219–224.